The Astrophysical Journal Letters, 898:L9 (6pp), 2020 July 20 https://doi.org/10.3847/2041-8213/aba0ae

Feasibility of Ion-cyclotron Resonant Heating in the Solar Wind

Roberto E. Navarro[1], Víctor Muñoz[2], Juan A. Valdivia[2], and Pablo S. Moya[2,3]
[1] Departamento de Física, Facultad de Ciencias Físicas y Matemáticas, Universidad de Concepción, Chile; roberto.navarro@udec.cl
[2] Departamento de Física, Facultad de Ciencias, Universidad de Chile, Chile; pablo.moya@uchile.cl
[3] Center for Mathematical Plasma Astrophysics, KU Leuven, Leuven, Belgium
Received 2020 May 1; revised 2020 June 27; accepted 2020 June 28; published 2020 July 17

Abstract

Wave–particle interactions are believed to be one of the most important kinetic processes regulating the heating and acceleration of solar wind plasma. One possible explanation for the observed preferential heating of alpha (He^{+2}) ions relies on a process similar to a second-order Fermi acceleration mechanism. In this model, heavy ions are able to resonate with multiple counter-propagating ion-cyclotron waves, while protons can encounter only single resonances, resulting in the subsequent preferential energization of minor ions. In this work, we address and test this idea by calculating the number of plasma particles that are resonating with ion-cyclotron waves propagating parallel and antiparallel to an ambient magnetic field $\boldsymbol{B}_0$ in a proton/alpha plasma with cold electrons. Resonances are calculated through the proper kinetic multispecies dispersion relation of Alfvén waves. We show that 100% of the alpha population can resonate with counter-propagating waves below a threshold $|\Delta U_{\alpha p}/v_A| < U_0 + a(\beta_p + \beta_0)^b$ in the differential streaming between protons and He^{+2} ions, where $U_0 = -0.532$, $a = 1.211$, $\beta_0 = 0.0275$, and $b = 0.348$ for isotropic ions. This threshold seems to match with constraints of the observed $\Delta U_{\alpha p}$ in the solar wind for low values of the plasma beta (β_p). Finally, it is also shown that this process is limited by the growth of plasma kinetic instabilities, a constraint that could explain alpha-to-proton temperature ratio observations in the solar wind at 1 au.

Unified Astronomy Thesaurus concepts: Solar wind (1534); Alfven waves (23); Plasma physics (2089)

1. Introduction

The mechanisms that heat the magnetically open corona and accelerate the fast solar wind plasma are still not well understood. Minor ions such as alpha particles (He^{+2}) flow away from the Sun faster than protons (Marsch et al. 1982; Feldman et al. 1996; Neugebauer et al. 1996; Steinberg et al. 1996; Marsch 2006), and are also preferentially heated to temperatures near mass proportionality (Kasper et al. 2008, 2013). Wave–particle interaction in plasmas is arguably one of the most important kinetic processes regulating the plasma dynamics via diffusion, heating, and acceleration in the solar wind (Seough et al. 2013; Wicks et al. 2016). The fact that most of the solar wind plasma has very low collisionality (Kasper et al. 2008; Bale et al. 2009; Verscharen et al. 2019) means that wave–particle interactions play an important role in the processes leading to plasma heating. Moreover, it has been shown that there is a strong correlation between kinetic instabilities driven by unstable particle velocity distribution functions (VDFs) and energy turbulent cascade rates in the solar wind at 1 au (Osman et al. 2012, 2013; Bruno & Carbone 2013).

In this context two recent models have been proposed for the preferential heating of alpha particles. Chandran et al. (2010) studied the stochastic interaction between ions and oblique low-frequency magnetic field fluctuations at their gyroradius scale. Stochastic heating occurs when an ion's orbit becomes chaotic due to obliquely propagating large-amplitude low-frequency fluctuations at the ion gyroscale, with amplitudes that in general decrease with scale size. Chandran et al. (2010) found that if Alfvénic turbulence is operating, alpha particles will be heated more effectively than protons because the associated fluctuations and gyroradius are larger at the alpha-gyroradius scale for similar temperatures. Also, they argued that imbalanced turbulent fluctuations, i.e., fewer waves propagating away from the Sun than toward it in the plasma frame, increase the likelihood of stochastic perpendicular heating.

Another possible mechanism for the heating of ions has been described by Isenberg (2001). In this proposal, protons are heated by cyclotron resonance while heavier ions can be heated by a second-order Fermi process due to multiple resonances with counter-propagating ion-cyclotron waves. In this model, resonating ions populate shells in velocity-space, and ions resonating simultaneously with forward and backward-propagating waves will be scattered rapidly by the resonant interaction. This mechanism allows ions to be transported between resonant shells, resulting in transverse heating of ions with respect to the magnetic field (Isenberg 2001; Isenberg & Vasquez 2007).

Recently, Kasper et al. (2013) showed evidence for strong transverse alpha particles heating in the solar wind for small differential streaming between alphas and protons, $\Delta U_{\alpha p}$. They also suggested that this preferential heating is constrained by values of $\Delta U_{\alpha p}$ below which test alpha particles can resonate with counter-propagating waves following the cold dispersion relation for Alfvén waves in an electron–proton plasma, $\omega = v_A k\sqrt{1 - \omega/\Omega_p}$, where ω, k, v_A, and Ω_p are the frequency, wavenumber, Alfvén speed, and proton-gyrofrequency, respectively. They found two possible velocity thresholds for this model: (a) $|\Delta U_{\alpha p}|/v_A < 0.168$ where the core of the alphas VDF experiences significant heating toward $T_{\perp\alpha}/T_{\perp p} \simeq 7$ by multiple resonances, where $T_{\perp s}$ correspond to $s =$ alphas and $s =$ protons perpendicular temperatures; and (b) $|\Delta U_{\alpha p}|/v_A > 0.168 + u_{\parallel\alpha}/v_A$ where the alpha particles become nonresonant, with $u_{\parallel\alpha}$ the alpha's parallel thermal speed. Beyond these thresholds preferential strong heating is limited and the average $T_{\perp\alpha}/T_{\perp p}$ ratio is observed to drop below 4.

It is worth noting that alpha particles are not necessarily test constituents of the solar wind. The fraction of alpha particles with respect to protons has been observed to be between 0.02 and 0.08 during high-speed streams (Steinberg et al. 1996). So, alphas represent almost 20% of the solar wind mass density, and their presence splits the Alfvén-cyclotron branch around the alpha gyrofrequency into a lower and an upper branch (Gomberoff & Cuperman 1982; Isenberg 1984; Viñas et al. 2014). This gap can be closed if thermal effects (Isenberg 1984) or nonzero values of $\Delta U_{\alpha p}$ (Gomberoff & Elgueta 1991) are considered, allowing the alphas to resonate with both branches continuously (Moya et al. 2013).

In this Letter, following the theoretical approach of Isenberg & Vasquez (2007) and Kasper et al. (2013), the number of plasma particles resonating simultaneously with counter-propagating electromagnetic waves is studied. Here, however, we use the proper kinetic dispersion relation of electromagnetic waves propagating along a background magnetic field in a plasma composed of a dense bi-Maxwellian proton core, a tenuous bi-Maxwellian alpha beam, and cold electrons. Through these calculations we show that there exists a threshold in $\Delta U_{\alpha p}$, below which 100% of the total alpha population can resonate with multiple waves, and that such process is limited by plasma kinetic instabilities arising at high values of the plasma beta. Finally, in the conclusions we discuss the implications of our results for the understanding of solar wind observations.

2. Theoretical Model: Resonances in a Kinetic Plasma

We consider a magnetized plasma composed of protons ($s = p$), alpha particles ($s = \alpha$), and cold electrons ($s = e$). The kinetic dispersion relation of left-handed circularly polarized electromagnetic waves propagating along the background magnetic field $\boldsymbol{B}_0$ is given by

$$c^2k^2 = \omega^2 + \sum_s \omega_{ps}^2[A_s + (A_s\xi_s^- + \xi_s)Z(\xi_s^-)], \qquad (1)$$

where ω is the complex wave frequency, k is the wavenumber along $\boldsymbol{B}_0$, and c is the speed of light. The summation is performed over all species s; $\omega_{ps} = \sqrt{4\pi q_s^2 n_s/m_s}$ is the plasma frequency; $A_s = R_s - 1$, where $R_s = T_{\perp s}/T_{\parallel s}$ is the temperature anisotropy; $T_{\perp s}$ and $T_{\parallel s}$ are the temperatures perpendicular and parallel with respect to $\boldsymbol{B}_0$, respectively; $\xi_s = (\omega - kU_s)/ku_{\parallel s}$ and $\xi_s^- = (\omega - kU_s - \Omega_s)/ku_{\parallel s}$ are resonance factors (Gary & Tokar 1985); U_s is the bulk speed; $u_{\parallel s} = \sqrt{2k_B T_{\parallel s}/m_s}$ is the parallel thermal speed; and $\Omega_s = q_s B_0/m_s c$ is the gyrofrequency. $Z(\xi)$ is the plasma dispersion function (Fried & Conte 1961). We also define the parallel $\beta_s = u_{\parallel s}^2/v_A^2$ and the Alfvén speed $v_A = B_0/\sqrt{4\pi\sum_s n_s m_s}$.

For the solar wind at 1 au, the alpha-to-proton density ratio is $n_\alpha/n_p \approx 0.05$, and the Alfvén speed is $v_A/c \approx 2 \times 10^{-4}$. For low frequencies, we can safely approximate $Z(\xi_e^-) \approx -1/\xi_e^-$ for cold electrons. The density n_e and bulk speed U_e of electrons are calculated by imposing charge neutrality ($\sum_s q_s n_s = 0$) and zero current ($\sum_s q_s n_s U_s = 0$). All results are shown in the center-of-mass reference frame ($\sum_s m_s n_s U_s = 0$).

Figure 1 shows three branches of $\omega(k)$ that solve the dispersion relation Equation (1) for $\beta_p = \beta_\alpha = 0.01$, $R_p = R_\alpha = 1$, and $\Delta U_{\alpha p}/v_A = \{0.0, 0.3\}$, where $\Delta U_{\alpha p} = U_\alpha - U_p$. The addition of alpha particles splits the Alfvén-cyclotron branch into the alpha-cyclotron (solid black line) and proton-cyclotron (dashed black line) branches. Gray lines are the forward and backward magnetosonic modes.

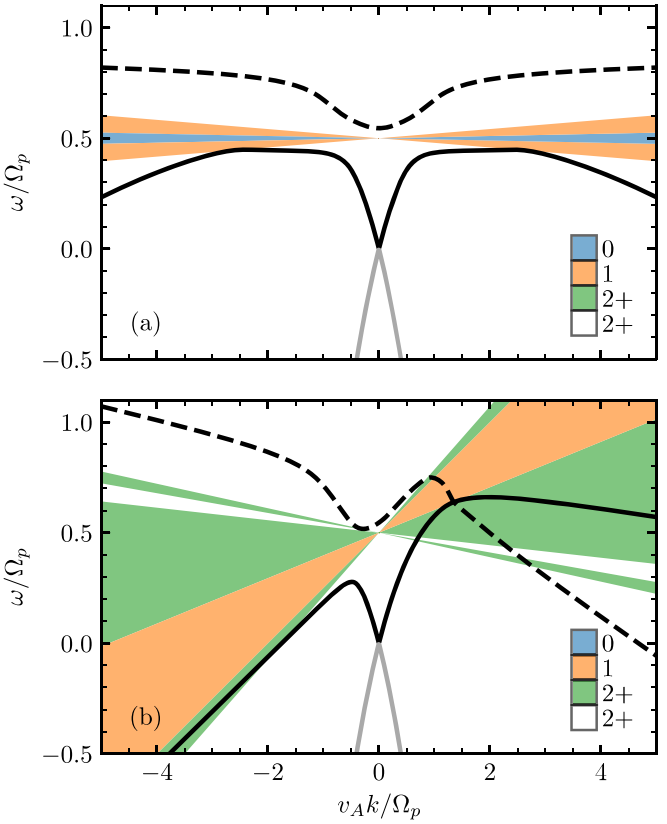

Figure 1. Solutions of the dispersion relation Equation (1) for $\beta_p = \beta_\alpha = 0.01$, $R_p = R_\alpha = 1$, and (a) $\Delta U_{\alpha p}/v_A = 0.0$ and (b) $\Delta U_{\alpha p}/v_A = 0.3$. Solid black, dashed black, and gray curves are the alpha-cyclotron, proton-cyclotron, and magnetosonic branches, respectively. Colored areas represent ranges of velocity $v_{\parallel\alpha}$ given by Equation (2), for which an alpha particle resonates with no waves (blue area) or one wave (orange area), and with co-propagating (green area) or counter-propagating waves (white area).

In the cold plasma limit the alpha- and proton-cyclotron branches approach asymptotically to $\omega = \Omega_\alpha = \Omega_p/2$ and $\omega = \Omega_p$, respectively, for $v_A k/\Omega_p \gg 1$. However, when kinetic effects are taken into account, the alpha-cyclotron branch bends at $v_A|k|/\Omega_p \simeq 2.5$ for $\beta_\alpha = \beta_p = 0.01$ (as shown in Figure 1(a)). For $\beta_s = 0.001$, this bending occurs at $v_A k/\Omega_p \simeq 5$. Thus the alpha-cyclotron branch is no longer asymptotic to $\omega = \Omega_\alpha$ even for small values of β_s. The proton-cyclotron branch does not seem to be affected by kinetic effects until $\beta_s \simeq 0.05$. Still, for large β_s, this branch seems to be asymptotic to some frequency between Ω_α and Ω_p.

For all values of β_s, R_s, and $\Delta U_{\alpha p}$, the proton-cyclotron branch crosses $k = 0$ at a cutoff frequency $\omega_c = \Omega_p(1 + 4n_\alpha/n_p)/(2 + 4n_\alpha/n_p) > \Omega_\alpha$. If $\Delta U_{\alpha p} = 0$, a frequency gap between Ω_α and ω_c is created, implying that alphas can at most be resonantly accelerated up to the proton velocity (Gomberoff & Cuperman 1982). However, this gap can disappear if thermal effects (Isenberg 1984) or $\Delta U_{\alpha p} \neq 0$ (Gomberoff & Elgueta 1991; Moya et al. 2013) are considered.

Figure 1(b) shows that the frequencies $\omega(k)$ are not symmetrical with respect to $k = 0$ for $\Delta U_{\alpha p} \neq 0$, such that the gap has disappeared, and the conditions for preferential

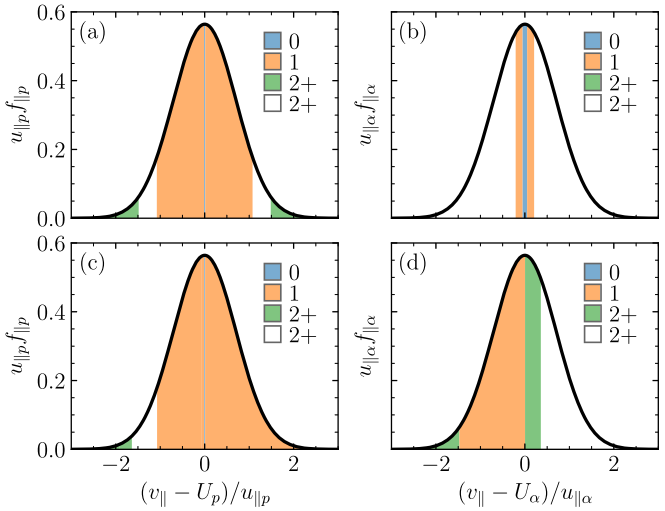

Figure 2. Portions of the Maxwellian VDF of (a) protons and (b) alphas resonating with modes of Figure 1(a) [$\Delta U_{\alpha p} = 0$]. Panels (c) and (d) show the same but for parameters in Figure 1(b) [$\Delta U_{\alpha p}/v_A = 0.3$]. Distributions are plotted in each species frame and normalized with respect to their thermal speeds. Color labels represent the VDF portions that are nonresonant (blue), resonant with a single wave (orange), and resonant with multiple co-propagating (green) or multiple counter-propagating waves (white).

resonant acceleration are recovered (Isenberg & Vasquez 2007). The dispersion relation Equation (1) also supports an infinite set of sound-like heavily damped modes (Astudillo 1996; Navarro et al. 2014), which we ignore here as we expect that they will not contribute to the heating of particles.

A particle of species s moving with velocity $v_{\|s}$ along $\boldsymbol{B}_0$ will be in cyclotron resonance if its gyrofrequency matches the Doppler-shifted frequency of the parallel-propagating electromagnetic wave, or

$$\omega(k) - kv_{\|s} = \Omega_s. \tag{2}$$

The resonance criterion Equation (2) is a straight line in Figure 1 intersecting $\omega(0) = \Omega_s$ with slope $v_{\|s}$. A particle will resonate if this line crosses the dispersion curve $\omega(k)$ given by Equation (1). Considering all k values up to $v_A k_{\max}/\Omega_p = \pm 80$, Figure 1 shows that, for alpha particles, there are velocities $v_{\|\alpha}$ in which Equation (2) does not cross the dispersion curve (blue areas) or crosses it only once (orange areas). Outside these areas, alpha particles will be able to resonate with multiple waves. In Figure 1 we distinguish between multiple resonances with co-propagating waves only (green areas) and with counter-propagating waves (white areas). Multiple resonances will scatter the particles so that they accelerate in the direction perpendicular to the wave propagation, in a process similar to a second-order Fermi mechanism (Isenberg & Vasquez 2007). This effect will be efficient whenever the resonant waves are counter-propagating, where the phase-speed difference is on the order of twice the Alfvén speed.

Figure 2 shows the portion of the proton and alpha VDFs that can resonate with zero (blue area), one (orange), co-propagating (green), or counter-propagating waves (white) whose frequencies are given by the modes shown in Figure 1. Figure 2(a) shows that, for $\Delta U_{\alpha p} = 0$, only the particles on the tails of the proton VDF are able to experience multiple resonances by either co-propagating or counter-propagating modes of Figure 1(a). This occurs only when fast protons can resonate with magnetosonic waves. Most of the proton VDF (85.84%) can experience only single resonances, thus proton energization in this case is limited. On the contrary, 76.89% of the alphas can resonate with counter-propagating waves in this case (see Figure 2(b)). Since multiple resonance is almost not available to protons for low beta and $\Delta U_{\alpha p} = 0$, and since most of the alpha population can resonate with counter-propagating waves, then heating by a second-order Fermi mechanism is preferential and more efficient on alphas than on protons.

For $\Delta U_{\alpha p} = 0.3$, the portion of protons resonating with co-propagating or counter-propagating waves is reduced to 6.50% and limited to the negative speed tail (compare Figures 2(a) and (c)). Figure 2(d) shows that the portion of the alpha VDF undergoing multiple resonances has decreased to 47.14%, and corresponds to particles with velocities $v_{\|\alpha} > U_\alpha$ and to particles in the negative speed tail. If heating by multiple resonances happens, then the alpha's VDF should develop a strong thermal anisotropy in the half $v_{\|\alpha} > U_\alpha$ part of the distribution, a feature that has been observed in hybrid simulations (Hellinger & Trávníček 2006).

It is important to mention that a different value of R_s, β_s, or $\Delta U_{\alpha p}$ will change the properties of the solutions $\omega(k)$ of the dispersion relation Equation (1). For high values of $\beta_s > 1$, the alpha- and proton-cyclotron branches are highly damped for $v_A k/\Omega_p > 1$ and not necessarily asymptotic to $\omega = \Omega_s$. For $R_s \neq 1$, the plasma may develop a magnetosonic (Gary et al. 2000) or ion-cyclotron (Gary et al. 2003) instability; and for $\Delta U_{\alpha p} \neq 0$, proton/alpha beam instabilities may arise (Araneda et al. 2002; Hellinger & Trávníček 2006; Verscharen et al. 2013).

Ignoring damping effects, in Figure 3 we show the portion of the proton and alpha VDFs that can resonate with counter-propagating waves (white areas in Figure 2), for different values of $\beta_p = \beta_\alpha$ (equal parallel thermal speeds), and relative drift $\Delta U_{\alpha p}/v_A$. In this figure, we consider isotropic VDFs, $R_p = R_\alpha = 1$. We have restricted the calculation to differential streams far from the kinetic instabilities, which are computed numerically through the dispersion relation Equation (1) by setting $(\mathrm{Im}\,\omega/\Omega_p)_{\max} = 10^{-4}$ as the instability thresholds.

In Figure 3(a), we observe that less than 10% of the proton VDF resonates with counter-propagating waves for most values of β_p and $\Delta U_{\alpha p}$. This means that heating by a second-order Fermi mechanism is likely not operating on protons in any observable case, but single cyclotron resonant heating can be expected. Kasper et al. (2013) use this argument to support the observed solar wind $R_p > 1$ values for $|\Delta U_{\alpha p}/v_A| > 0.168 + \sqrt{\beta_p}$ and $\beta_p < 1$. Kasper et al. (2013) have also reported that observations with $T_{\perp\alpha}/T_{\perp p} \approx 7$ are constrained by the threshold $|\Delta U_{\alpha p}/v_A| < 0.168$ (shown in Figure 3(b) with white dotted lines). Our analysis shows that inside these lines more than half of the alpha population is susceptible to strong resonant heating by counter-propagating waves.

The suggestion proposed by Kasper et al. (2013) may apply only for $\beta_p \lesssim 0.2$ where a cold plasma model is a relatively good approximation to the kinetic plasma dispersion relation Equation (1) (Cuperman et al. 1975; Cuperman & Gomberoff 1977; Gomberoff & Vega 1989). For $\beta_p > 0.2$ kinetic effects are predominant and the thresholds for strong multiple resonances to occur are modified toward higher values of $|\Delta U_{\alpha p}|$. In Figure 3(b), the purple area indicates that all alpha

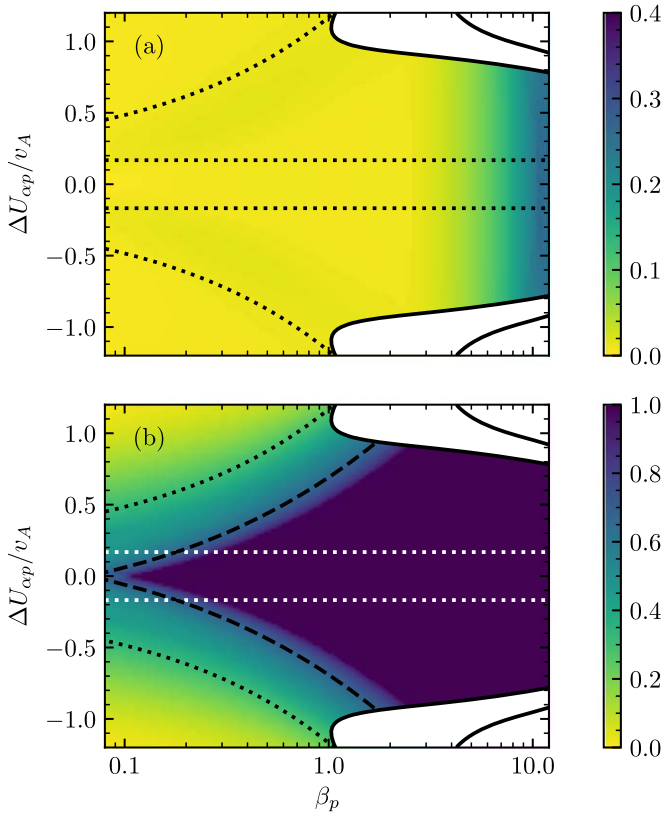

Figure 3. Portion P_s (see the color scale) of the total VDF of (a) protons and (b) alpha particles undergoing multiple resonances with counter-propagating waves, as a function of parallel β_p and drift $\Delta U_{\alpha p}$, considering $\beta_\alpha = \beta_p$ and $R_p = R_\alpha = 1$. Color bars in (a) and (b) are different. Dotted lines correspond to the $|\Delta U_{\alpha p}|/v_A = 0.168$ and $|\Delta U_{\alpha p}|/v_A = 0.168 + \sqrt{\beta_p}$ thresholds suggested by Kasper et al. (2013). Dashed lines are contour lines, where $P_s = 0.68$ (one standard deviation of VDF). White areas correspond to regions where an instability $\mathrm{Im}\,\omega > 0$ develops. Solid lines are the contours for $(\mathrm{Im}\,\omega/\Omega_p)_{\max} = \{10^{-4}, 10^{-3}\}$.

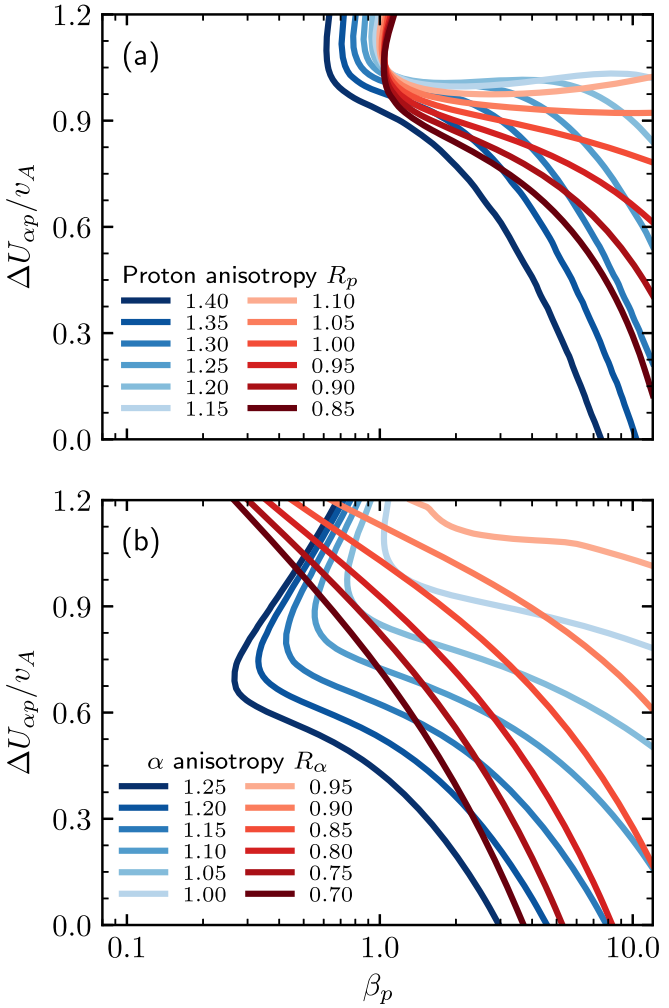

Figure 4. Contours of the maximum growth rate $(\mathrm{Im}\,\omega/\Omega_p)_{\max} = 10^{-4}$ as a function of $\beta_p = \beta_\alpha$ and $\Delta U_{\alpha p}/v_A > 0$ for (a) fixed $R_\alpha = 1.0$ and varying R_p; and (b) vice versa. Plots for $\Delta U_{\alpha p}/v_A < 0$ can be obtained by mirroring these figures with respect to the β_p axis.

particles (100% of the VDF) are resonating with counter-propagating waves. This area is constrained by the long-dashed curve, which is simply a contour line in which 68% of the alpha VDF experiences multiple resonances. This boundary can be fitted by a power-law function of the form

$$\frac{\Delta U^*}{v_A} = U_0 + a(\beta_p + \beta_0)^b, \tag{3}$$

where $U_0 = -0.532$, $a = 1.211$, $\beta_0 = 0.0275$, and b=0.348.

For $|\Delta U_{\alpha p}| > \Delta U^*$, alphas with velocities $v_{\parallel\alpha} > \Delta U_{\alpha p}$, i.e., less than half the VDF, are susceptible to multiple resonances. For comparison purposes, we have included in Figure 3(b) the threshold $|\Delta U_{\alpha p}|/v_A = 0.168 + u_{\parallel\alpha}/v_A$ derived by Kasper et al. (2013) with a dotted black line. So, Equation (3) represents a generalization of the limit suggested by Kasper et al. (2013). It is interesting to note that these thresholds are similar to the upper bound limits of the differential streaming $\Delta U_{\alpha p}$ observed in the solar wind for low β_α (Bourouaine et al. 2013), suggesting that multiple resonances could also be related to the acceleration of the alpha particles with respect to the protons.

The white areas in Figure 3 correspond to values of β_p and $\Delta U_{\alpha p}$ for which the plasma develops kinetic instabilities with $(\mathrm{Im}\,\omega/\Omega_p)_{\max} > 10^{-4}$. Kasper et al. (2013) noticed a drop in the average value of $T_{\perp\alpha}/T_{\perp p} \approx 7$ toward 4 for $\beta_p > 2$. This probably occurs because the plasma is regulating itself due to instabilities and, as pointed out by Bourouaine et al. (2013), the observed $\Delta U_{\alpha p}$ is probably constrained for high β_α by kinetic instabilities as the ones shown in Figure 3.

Qualitatively speaking, the thresholds of multiple resonances for values of $R_\alpha \neq 1$ or $R_p \neq 1$ are not much different from Figure 3. A fit of Equation (3) for $R_p = 0.9$ and $R_\alpha = 1.1$ results in $U_0 = -0.693$, $a = 1.411$, $\beta_0 = 0.0491$, and $b = 0.322$, whose boundaries almost completely overlap on top of the one calculated for $R_p = R_\alpha = 1$ in Figure 3. Thus, in Figure 3 we only show the isotropic case. Yet, the instability thresholds can change considerably. Figure 4 shows the instability thresholds with growth rate $\gamma/\Omega_p = 10^{-4}$ as a function of $\beta_p = \beta_\alpha$ and $\Delta U_{\alpha p}/v_A > 0$. In Figure 4(a), $R_\alpha = 1$ is kept constant. We see that the instability thresholds shift to higher values of β_p and higher values of $\Delta U_{\alpha p}/v_A$ as the proton anisotropy lowers from $R_p = 1.40$ to $R_p \approx 1.15$. This description is reversed for lower values of $R_p \lesssim 1.15$. A similar behavior is seen when $R_p = 1$ is kept constant but R_α varies, as shown in Figure 4(b).

These instabilities are triggered by the combined effects of temperature anisotropy and relative drift (Wicks et al. 2016). Thus, for $R_p = R_\alpha = 1$, whenever $\Delta U_{\alpha p} \neq 0$ there is an effective anisotropy $R_{\mathrm{eff}} < 1$ that drives the proton/alpha beam

instability. The effective anisotropy grows toward $R_{\rm eff} = 1$ if either $R_p > 1$ or $R_\alpha > 1$ for $\Delta U_{\alpha p} \neq 0$. After a critical value (e.g., $R_p \simeq 1.15$), then $R_{\rm eff} > 1$, suggesting that a different instability may develop. This may explain the apparent reversal in the trends for the instability thresholds for $R_p \neq 1$ or $R_\alpha \neq 1$.

Although the density of alpha particles is much lower than protons, the instability thresholds are more sensitive to variations of R_α compared to R_p. It is worth mentioning that the dominant instability occurs for forward propagating waves in the alpha-cyclotron branch (solid black line with $k > 0$ in Figure 1) both for $R_p \gtrsim 0.90$ in Figure 4(a) and for $R_\alpha \gtrsim 0.95$ in Figure 4(b). Otherwise, the dominant instability is for backward-propagating waves in the alpha-cyclotron branch (solid black line with $k < 0$ in Figure 1).

3. Summary and Conclusions

We have calculated the percentage of plasma particles that resonate with counter-propagating cyclotron waves moving along an ambient magnetic field $\boldsymbol{B}_0$, in a proton/alpha plasma with cold electrons. The VDF of protons and alphas were considered as Bi-Maxwellian with relative drift along $\boldsymbol{B}_0$. Resonance percentages were calculated with the resonance condition $\omega(k) - k v_{\|s} = \Omega_s$, where $\omega(k)$ are the frequencies of the three main solutions (modes) of the exact kinetic dispersion relation, Equation (1). In this fully kinetic approach, we show that less than 10% of protons can resonate with multiple waves for most values of β_p and $\Delta U_{\alpha p}$ (see Figure 3(a)). For $\beta_p > 10$, the portion of resonant protons raises to 50% but the plasma may develop a kinetic instability in this region. Thus, we conclude that protons are unable to experience perpendicular heating by a second-order Fermi mechanism in most observable cases.

Our results also show that a large percentage, close to 100%, of the alpha population can resonate with counter-propagating waves below a threshold $\Delta U^* = U_0 + a(\beta_p + \beta_0)^b$. Since this process is not available to protons, heating by this mechanism is preferential to alpha particles (in general to heavier ions). Below this threshold, solar wind measurements show that alphas exceed mass-proportion temperatures with respect to protons (Kasper et al. 2013), suggesting that resonance with counter-propagating waves may play a role in the perpendicular heating of alpha particles. Above this threshold and for low values of β_p, the portion of the alpha population capable of experiencing second-order Fermi heating drops below 50%, suggesting that alpha particles may not be strongly heated in the perpendicular direction with respect to $\boldsymbol{B}_0$. Thus, for all the cases outside this threshold (e.g., anisotropic distributions in Figure 3 of Kasper et al. 2013) the relevant heating mechanism could be nonresonant, such as the stochastic heating studied by Chandran et al. (2010). However, surprisingly, values of $\Delta U_{\alpha p} > \Delta U^*$ seem to be forbidden in the solar wind (Bourouaine et al. 2013), raising the question of whether resonances are required to maintain the alphas at drifts below the threshold ΔU^*.

For high values of β_p the plasma develops a kinetic instability in the alpha-cyclotron branch. The threshold of this instability limits the possible values of $\Delta U_{\alpha p}$ (Bourouaine et al. 2013). However, Kasper et al. (2013) noticed a drop in $T_{\perp\alpha}/T_{\perp p} \to 4$ above the instability threshold. It can be argued that the plasma is regulating itself to lower the instability so that temperatures evolve toward mass proportionality.

Finally, we also show that even for a small density ratio $n_\alpha/n_p = 0.05$, the instability thresholds for $\Delta U_{\alpha p}$ are more sensitive to variations in the anisotropy of alpha particles compared to the proton anisotropy. Thus, alpha particles cannot be treated as test constituents of the solar wind plasma. Nevertheless, many open questions, such as the quantification of the presence of counter-propagating ion-cyclotron waves (Osman et al. 2013), still remain. New measurements from Parker Solar Probe or Solar Orbiter, as well as the use of quasilinear (Seough et al. 2013; Moya et al. 2014) or particle simulations (Araneda et al. 2009; Maneva et al. 2015) are necessary to further characterize the dominant physical processes, such as wave–wave interactions, or nonlinear effects, that regulate the observed state of the solar wind plasma.

We are grateful for the support of ANID, Chile, through FONDECyT grants No. 11180947 (R.E.N.), No. 1201967 (V. M.), No. 1190703 (J.A.V.), and No. 1191351 (P.S.M). R.E.N. is also thankful for the support of CONICyT-PAI No. 79170095, and P.S.M is thankful for the support of KU Leuven through the BOF Network Fellowship NF/19/001.

ORCID iDs

Roberto E. Navarro https://orcid.org/0000-0003-0782-1904
Víctor Muñoz https://orcid.org/0000-0003-1746-4875
Juan A. Valdivia https://orcid.org/0000-0003-3381-9904
Pablo S. Moya https://orcid.org/0000-0002-9161-0888

References

Araneda, J. A., Maneva, Y. G., & Marsch, E. 2009, PhRvL, 102, 175001
Araneda, J. A., Viñas, A. F., & Astudillo, H. F. 2002, JGRA, 107, 1453
Astudillo, H. F. 1996, JGR, 101, 24433
Bale, S. D., Kasper, J. C., Howes, G. G., et al. 2009, PhRvL, 103, 211101
Bourouaine, S., Verscharen, D., Chandran, B. D., Maruca, B. A., & Kasper, J. C. 2013, ApJL, 777, L2
Bruno, R., & Carbone, V. 2013, LRSP, 10, 2
Chandran, B. D. G., Li, B., Rogers, B. N., Quataert, E., & Germaschewski, K. 2010, ApJ, 720, 503
Cuperman, S., & Gomberoff, L. 1977, JPlPh, 18, 391
Cuperman, S., Gomberoff, L., & Sternlieb, A. 1975, JPlPh, 14, 195
Feldman, W., Barraclough, B., Phillips, J., & Wang, Y.-M. 1996, A&A, 316, 355
Fried, B. D., & Conte, S. D. 1961, The Plasma Dispersion Function: The Hilbert Transform of the Gaussian (San Diego, CA: Academic Press)
Gary, S. P., & Tokar, R. L. 1985, JGR, 90, 65
Gary, S. P., Yin, L., Winske, D., et al. 2003, JGRA, 108, 1068
Gary, S. P., Yin, L., Winske, D., & Reisenfeld, D. B. 2000, JGR, 105, 20989
Gomberoff, L., & Cuperman, S. 1982, JGR, 87, 95
Gomberoff, L., & Elgueta, R. 1991, JGR, 96, 9801
Gomberoff, L., & Vega, P. 1989, PPCF, 31, 629
Hellinger, P., & Trávníček, P. 2006, JGR, 111, A01107
Isenberg, P. A. 1984, JGR, 89, 2133
Isenberg, P. A. 2001, JGR, 106, 29249
Isenberg, P. A., & Vasquez, B. J. 2007, ApJ, 668, 546
Kasper, J. C., Lazarus, A. J., & Gary, S. P. 2008, PhRvL, 101, 261103
Kasper, J. C., Maruca, B. A., Stevens, M. L., & Zaslavsky, A. 2013, PhRvL, 110, 091102
Maneva, Y., Viñas, A. F., Moya, P. S., Wicks, R. T., & Poedts, S. 2015, ApJ, 814, 33
Marsch, E. 2006, LRSP, 3, 1
Marsch, E., Mühlhäuser, K.-H., Rosenbauer, H., Schwenn, R., & Neubauer, F. 1982, JGR, 87, 35
Moya, P. S., Navarro, R., Muñoz, V., & Valdivia, J. A. 2013, PhRvL, 111, 029001
Moya, P. S., Navarro, R., Viñas, A. F., Muñoz, V., & Valdivia, J. A. 2014, ApJ, 781, 76
Navarro, R. E., Moya, P. S., Muñoz, V., et al. 2014, PhRvL, 112, 245001

Neugebauer, M., Goldstein, B. E., Smith, E. J., & Feldman, W. C. 1996, JGR, 101, 17047
Osman, K. T., Matthaeus, W. H., Hnat, B., & Chapman, S. C. 2012, PhRvL, 108, 261103
Osman, K. T., Matthaeus, W. H., Kiyani, K. H., Hnat, B., & Chapman, S. C. 2013, PhRvL, 111, 201101
Seough, J., Yoon, P. H., Kim, K.-H., & Lee, D.-H. 2013, PhRvL, 110, 071103
Steinberg, J. T., Lazarus, A. J., Ogilvie, K. W., Lepping, R., & Byrnes, J. 1996, GeoRL, 23, 1183
Verscharen, D., Bourouaine, S., & Chandran, B. D. G. 2013, ApJ, 773, 163
Verscharen, D., Klein, K. G., & Maruca, B. A. 2019, LRSP, 16, 5
Viñas, A. F., Moya, P. S., Araneda, J. A., & Maneva, Y. G. 2014, ApJ, 786, 86
Wicks, R., Alexander, R., Stevens, M., et al. 2016, ApJ, 819, 6